ELSEVIER

Journal of Photochemistry and Photobiology
A: Chemistry 89 (1995) 177–189

Journal of PHOTOCHEMISTRY AND PHOTOBIOLOGY A: CHEMISTRY

Photoassisted hydrogen production from a water–ethanol solution: a comparison of activities of Au–TiO_2 and Pt–TiO_2

Gratian R. Bamwenda [1], Susumu Tsubota, Toshiko Nakamura, Masatake Haruta *

Osaka National Research Institute, AIST, Department of Energy and the Environment, Midorigaoka 1-8-31, Ikeda, 563 Osaka, Japan

Received 3 May 1994; accepted 10 January 1995

Abstract

A comparison of the photocatalytic activity for H_2 generation between Au–TiO_2 and Pt–TiO_2 has been made. The deposition of Au and Pt was carried out using TiO_2 powders in aqueous suspensions containing $HAuCl_4 \cdot 4H_2O$ or $H_2PtCl_6 \cdot 6H_2O$ by deposition–precipitation (DP), impregnation (IMP), photodeposition (FD) and, in the case of Au, by mixing TiO_2 with colloidal gold suspensions (MIX). The main reaction products obtained from the irradiation of an aqueous 5 M C_2H_5OH suspension containing Au–TiO_2 or Pt–TiO_2 were hydrogen, methane, carbon dioxide and acetaldehyde. Small amounts of acetic acid were also detected. The overall activity of Au samples was generally about 30% lower than that of Pt samples. The activity of Au samples strongly depended on the method of preparation and decreased in the order Au–TiO_2-FD > Au–TiO_2-DP > Au–TiO_2 -IMP > Au–TiO_2-MIX. The activities of the platinum samples were less sensitive to the preparation method and decreased in the order Pt–TiO_2-FD > Pt–TiO_2-DP ≈ Pt–TiO_2 -IMP. Gold and platinum precursors calcined in air at 573 K showed the highest activity towards H_2 generation, followed by a decline in activity with increasing calcination temperature. The H_2 yield was found to be dependent on the metal content on TiO_2 and showed a maximum in the ranges 0.3–1 wt.% Pt and 1–2 wt.% Au. The exposed surface area of gold had only a small influence on the rate of hydrogen generation. On the other hand, the rate of H_2 production was strongly dependent on the initial pH of the suspension. pH values in the range 4–7 gave better yields, whereas highly acidic and basic suspensions resulted in a considerable decrease in the H_2 yield.

Keywords: Photocatalysis; Water–ethanol; Hydrogen production; Catalyst preparation methods; Gold; Platinum; Titania

1. Introduction

During the last two decades, significant progress has been achieved in the use of integrated chemical systems based on semiconductor particulates in gaseous and liquid phase photoredox processes [1–5]. The particular advantages of semiconductor particulate systems can be summarized as follows: (a) they are inexpensive and relatively easy to make; (b) they can provide anodic and cathodic sites at different parts of the particulate surface; (c) they have a large surface area that facilitates light absorption and heterogeneous transfer of electrons and holes to solution species. These particulates, in the form of colloids and powder suspensions with or without metal deposits, can be used to carry out reactions that may be of use in wastewater treatment [6–12], and may also find valuable application in the photoproduction of hydrogen which is a potential candidate for a non-polluting source of energy [13,14]. To enhance the photoproduction of H_2 over semiconductor materials, particles of platinum, palladium, rhodium, copper and metal oxides, e.g. RuO_2, have been deposited on semiconductors, such as TiO_2, $SrTiO_3$, ZnO, WO_3, Fe_2O_3, CdS and others, mainly by photodeposition (FD) [15–23], impregnation (IMP) [24–29] and physical mixing [24,30].

It has been recognized recently that Au–TiO_2 is an active catalyst in thermal [31–36] and photochemical [37–41a] processes. In an earlier study [41a], we demonstrated that Au–TiO_2 particles, prepared by deposition–precipitation (DP), can be used in the production of H_2 from an aqueous ethylene glycol suspension. The amount of H_2 produced was found to be dependent on the catalyst treatment conditions, initial pH and concentration of ethylene glycol, and slightly dependent on the reaction temperature and details of the surface structure. In a recent study [41b], we found that Au–TiO_2

* Corresponding author.

[1] Present address: National Institute for Resources and Environment, Environmental Technology Division, 16-3 Onogawa, Tsukuba, Ibaraki 305, Japan.

SSDI 1010-6030(95)04039-0

prepared by DP exhibited a higher activity for heterogeneous CO oxidation than Pt–TiO_2, whereas platinum catalysts prepared by FD and IMP showed a better activity than the corresponding Au–TiO_2. In addition, the activity for CO oxidation was strongly dependent on the preparation method in the case of Au–TiO_2 and insensitive in the case of Pt–TiO_2. These findings prompted the undertaking of a study to compare the photocatalytic activity of Au–TiO_2 and Pt–TiO_2 catalysts which have been used frequently in previous H_2 production studies.

The catalysts used in this study were prepared by FD, DP, IMP and by mixing TiO_2 with colloidal gold suspended in α-terpineol (MIX). Several parameters that affect H_2 production were studied, such as the catalyst preparation methodology, metal content, morphology of metal particles, pH and duration of illumination. Our experimental configuration allowed us to compare the activities of various catalysts, since the photon flow, geometry of the reactor, height and amount of suspension were kept constant. Ethanol was chosen as a sacrificial agent because C_1–C_3 alcohols in water–alcohol mixtures are satisfactory hole scavengers and, in addition, they undergo a relatively rapid and irreversible oxidation [18,24,25,28,42,43].

Although it is difficult to compare quantitatively our results with the data on H_2 yields obtained from the literature due to differences in the catalyst preparation methods, irradiation geometries and/or sources, a comparison is made when it is appropriate.

2. Experimental details

2.1. Materials

Powdered TiO_2 (better than 99.5%, P-25, Japan Aerosil Co.) was primarily anatase with a surface area of 50 $m^2\ g^{-1}$. The reagents $HAuCl_4 \cdot 4H_2O$, $H_2PtCl_6 \cdot 6H_2O$ and ethyl alcohol (Kishida Chemicals) were all of 99.5% purity. NaOH, H_2SO_4 and hydrochloric acid were of high purity and were used without further purification. The impurity levels of noble metals in chloroauric acid were approximately 2, 7 and 11 ppm for platinum, iridium and palladium respectively, as determined by atomic emission spectroscopy. A 10 wt.% gold colloid with a mean diameter of 5 nm, dispersed in α-terpineol, was obtained from Shinkuyakin Co. Ltd.

2.2. Catalyst preparation

2.2.1. Photodeposition

The procedure used for the photochemical deposition of Au and Pt onto TiO_2 is similar to that reported by Kraeutler and Bard [15]. The TiO_2 (100 mg) was dispersed in 4 cm^3 of distilled water by ultrasonic agitation for 1 h. Following sonication, the slurry was transferred to the reactor, and a solution of 1 : 1 (v/v) water–methanol was added so that the final volume was about 50 cm^3. Subsequently, the required amounts of aqueous solutions of $HAuCl_4 \cdot 4H_2O$ or $H_2PtCl_6 \cdot 6H_2O$ were added. Small amounts of NaOH solution were then added to adjust the pH of the suspension to the required values. The mixture was then deaerated with pure argon (75–80 $cm^3\ min^{-1}$) for 30 min with magnetic stirring. After deaeration, the suspension was irradiated with a 125 W high pressure Hg lamp (Ushio), operated at 25 mW cm^{-2} and 313 K, for a period sufficient for deposition of most of the metal (0.5–1 h). After irradiation, the metal–TiO_2 was removed from the reaction mixture by filtration through a 0.15 μm Millipore filter, washed four times in hot distilled water for Cl^- removal, and the resulting paste was vacuum dried for 15 h. During the FD of Au and Pt, small amounts of H_2 in the range 0.3–0.45 mmol were also produced. Samples prepared by FD are denoted metal–TiO_2-FD.

2.2.2. Deposition–precipitation

The deposition of platinum and gold by DP was carried out as follows [31]. Aqueous solutions of chloroauric or chloroplatinic acid were heated to 343 K and their pH was adjusted to the required value by the addition of small amounts of 0.1 or 1 M NaOH. This was followed by the addition of appropriate amounts of TiO_2 (1–3 g). The slurry was then aged for 1 h, after which it was washed in 2 dm^3 of distilled water, decanted and the cleaning procedure was repeated six times. The resulting material was vacuum dried at 0.4 Pa for 15 h and then calcined in air at temperatures between 673 and 773 K for 4 h. The calcined samples were transferred to a U-shaped quartz tube, flushed with pure argon (80 $cm^3\ min^{-1}$) while raising the temperature and finally reduced in flowing H_2 (1 vol.% in N_2, 80 $cm^3\ min^{-1}$) at 723 K for 10–20 h, followed by cooling to room temperature under an argon flow. The samples were then ground and sieved into 44/74 μm fractions. Before calcination, Pt–TiO_2 catalysts had a white colour. On calcination, they acquired a light khaki colour that turned to a dark grey tint after H_2 treatment. The appearance of Au–TiO_2 samples changed from light purple to dark purple after calcination. There was no significant variation in the appearance of Au–TiO_2 samples after H_2 treatment. The samples prepared by DP are denoted as 1%metal–TiO_2-DP to indicate the metal content, type of metal, titania and method of preparation.

2.2.3. Impregnation

For catalysts prepared by IMP, a known amount of TiO_2 (1–2 g) was suspended in 20 cm^3 aliquots of aqueous $HAuCl_4 \cdot 4H_2O$ or $H_2PtCl_6 \cdot 6H_2O$. This was followed by evaporation to dryness in a rotary evaporator

at 313 K under reduced pressure. The remaining paste was dried and subsequently calcined in air at 673 K for 4 h, and then reduced in flowing H_2 at 723 K for 10 h according to the procedure described above. Impregnated samples are identified by the code metal–TiO_2-IMP.

2.2.4. Physical mixing

For Au–TiO_2 samples prepared from colloidal gold [31b], TiO_2 (5 g) was added to an Au colloidal suspension in α-terpineol and then diluted with isopropyl ether to obtain the final desired Au concentration. The solvent was evacuated at 373 K for 4 h and the remaining solid was calcined in air at 473 or 873 K for 4 h. These samples are designated as Au–TiO_2-MIX.

2.2.5. Unsupported TiO_2 samples

On the suggestion of the referee, we prepared unsupported TiO_2-DP, TiO_2-FD, TiO_2-IMP and TiO_2-MIX. These materials were prepared and pretreated in identical fashion to the corresponding Au–TiO_2 and Pt–TiO_2 samples, but without the incorporation of the metal.

2.3. Apparatus and procedures

Experiments were performed in a cylindrical quartz photoreactor of 120 cm^3 capacity. The top of the reactor was equipped with a gas-tight silicon septum for gas phase sampling and two side-arm stopcocks that permitted argon bubbling. Water was circulated through the reactor jacket in order to maintain a constant temperature. Illumination of the suspension was carried out with a 500 W high pressure mercury arc lamp (Ushio USH-500D) operated at an incident flux of 30 mW cm^{-2}. The wavelength of the UV light reaching the suspension was in the range 276–342 nm. The incident light flux was measured by a radiometer (Topcon UVR-36).

A TiO_2 sample (50 mg) with supported Au or Pt was suspended in 30 cm^3 of an aqueous solution of 5 M C_2H_5OH. A concentration of 5 M C_2H_5OH was chosen because our earlier study [41a] had shown that this concentration is adequate for long-term irradiation experiments. The suspension was then flushed with argon for 30 min to remove physisorbed gases. After degassing, the reactor was closed and the suspension was allowed to stabilize for 15 min in the dark. The experiment was started by illumination of the suspension, with continuous stirring, at 310 ± 1 K and atmospheric pressure. The course of the reaction was monitored by periodic sampling of the gas phase (50–100 μl gas aliquots).

Hydrogen was analysed by gas chromatography (GC) using a Shimadzu GC-8A equipped with a thermal conductivity detector (TCD) and a stainless steel column (2 m) packed with molecular sieves (13X) at 323 K. Argon was used as carrier gas at a flow rate of 20 cm^3 min^{-1}. Several reproducibility tests were performed with various catalyst samples. The uncertainty in the measurement of the H_2 yields was found to be less than 5%. Methane and carbon dioxide were determined by GC using a Yanaco G2800 gas chromatograph with a Porapak Q column (2 m) at 333 K and a TCD. Helium was used as carrier gas at a flow rate of 40 cm^3 min^{-1}. Calibration was performed with standard gas samples. Mass spectral analyses of the gaseous products were carried out using an MMC-100 Ulvac mass spectrometer.

Liquid products were analysed as follows. After irradiation for a given interval, in the manner described above, the metal–TiO_2 particles in the suspension were filtered and the filtrate was analysed using a Shimadzu 14A gas chromatograph with a 50 m H2Om-PW50-300 capillary column (Shinwa Chemicals) and a flame ionization detector. The identification of the liquid products was performed using gas chromatography–mass spectrometry (GC–MS) (Hitachi M-2000).

Except for the samples prepared by physical mixing, the amount of metal deposited on TiO_2 was determined both by X-ray fluorescence (Rigaku 3370 analyser) and inductively coupled plasma spectrometry (ICP-AES) (Seiko SPS 1200 VR). The amount of Cl^- in the catalyst samples was determined, after dissolution, by ion chromatography (Nippon Dyomex 2000i). Transmission electron micrographs of Au–TiO_2 and Pt–TiO_2 samples were obtained with a Hitachi H-9000 microscope. The sizes of the metal particles were measured using a computerized image analyser (Excel, Nippon Avionics Co. Ltd.). The size distribution of the gold and platinum crystallites was determined by measuring 100–600 crystallites for each sample.

3. Results

3.1. Catalyst characterization

Fig. 1 shows the transmission electron micrographs of samples prepared by DP and FD. It can be seen that the Au and Pt particles are well dispersed on TiO_2. Small metal particles in the range 1–10 nm were obtained for Au–TiO_2-FD and Au–TiO_2-DP and in the range 1–6 nm for Pt–TiO_2-FD, Pt–TiO_2-DP and Pt–TiO_2-IMP, as shown by the size distribution histograms in Fig. 2. In addition, for the same loading, the sizes of the Pt crystallites were usually slightly smaller than those observed for the gold samples. It is also worth noting that the size distribution of Au particles is usually symmetrical, independent of the preparation method (see Fig. 2). In the case of Pt, the crystallites have a narrow size distribution and their

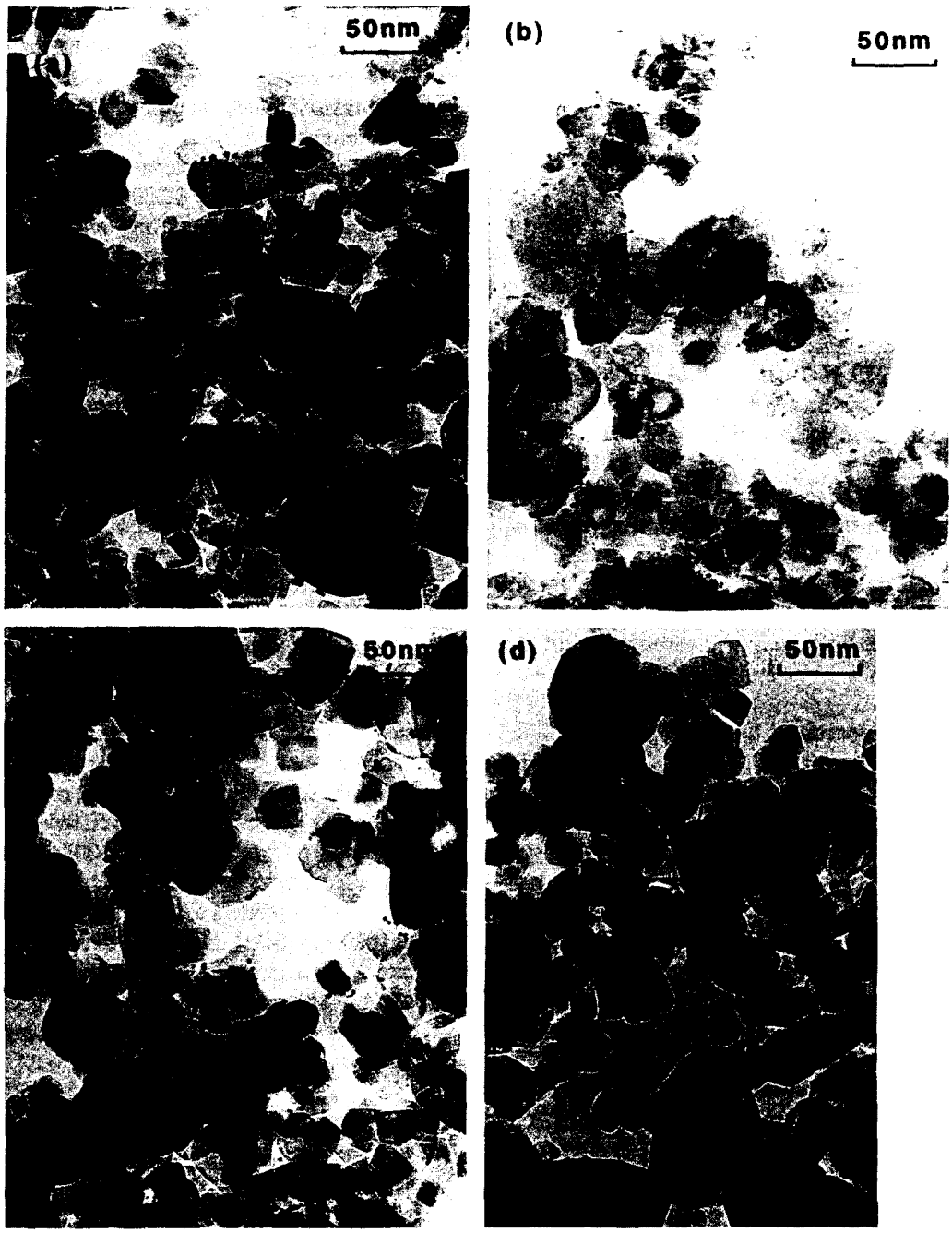

Fig. 1. Transmission electron micrographs of catalyst samples showing Au and Pt particles deposited on TiO_2 grains by the photodeposition (FD) and deposition–precipitation (DP) methods. The DP samples were calcined in air at 673 K for 4 h and then reduced in H_2 at 723 K for 10 h. (a) 1wt.%Au–TiO_2-FD; (b) 2.2wt.%Au–TiO_2-DP; (c) 1wt.%Pt–TiO_2-FD; (d) 0.5wt.%Pt–TiO_2-DP. Magnification, 400 000×.

sizes are shifted towards smaller diameters in the DP method and are symmetrical for FD and IMP. The mean diameters of the Au particles in Au–TiO_2-MIX were 5.1 ± 1.3 nm and 11.6 ± 2.5 nm for samples calcined at 473 K and 873 K respectively. No significant change was observed in the mean diameter or size distribution of the deposited metal particles after H_2 production experiments. Fig. 3 shows a high resolution transmission electron micrograph of Au particles in a 3.3wt.%Au–TiO_2-DP sample, indicating that Au crystallites are deposited on TiO_2 as hemispherical particles with the flat face towards the TiO_2 surface.

In the photochemical deposition method (FD), on irradiation, the colour of the suspension changed from white to purple and dark grey for $HAuCl_4$–TiO_2 and H_2PtCl_6–TiO_2 suspensions respectively, indicating the deposition of metal Au and Pt on the TiO_2 particles. The data referring to FD are summarized in Table 1. Several preliminary runs were performed in order to determine the deposition conditions, such as the light

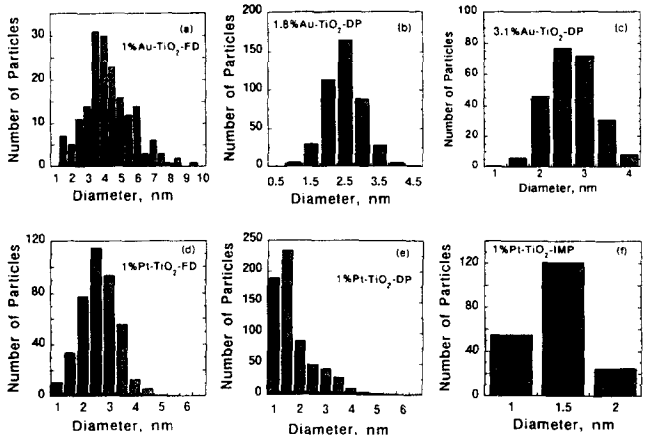

Fig. 2. Size distribution of Au and Pt particles deposited on TiO_2.

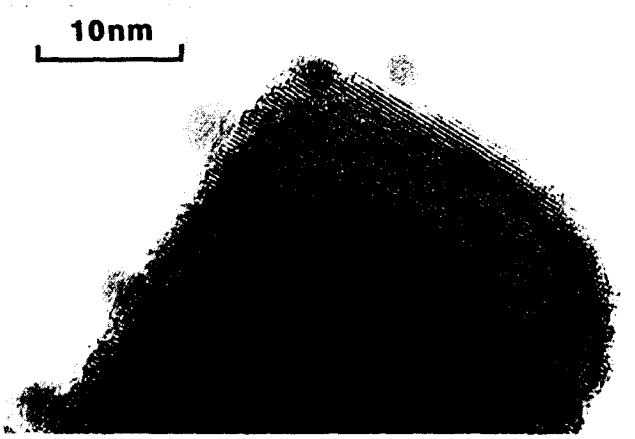

Fig. 3. High resolution electron micrograph showing Au particles on the surface of a TiO_2 grain. Loading is 3.3 wt.% Au.

Table 1
Parameters for gold and platinum photodeposition (FD) on TiO_2 (100 mg TiO_2 powder in 50 cm^3 stirred suspension containing 1 : 1 (v/v) CH_3OH : H_2O and $HAuCl_4 \cdot {}_2O$ or $H_2PtCl_6 \cdot 6H_2O$ under argon; light source, 125 W Hg lamp operated at 25 mW cm^{-2}; temperature, 310 K)

Experiment/ suspension	Concentration [a] (mg dm^{-3})	pH_0	$t_{deposition}$ (h)	Loading (wt.%)	d [b] (nm)
$HAuCl_4$–TiO_2					
1	22	7	1	0.5	5.0±1.8
2	43	7	0.5	0.98	4.6±1.5
3	43	7	1	1.1	n.d. [c]
4	43	7	4	1.2	n.d.
5	86	7	1	2.35	n.d.
H_2PtCl_6–TiO_2					
6	27	4	1	0.46	2.6±0.9
7	54	4	1	1	2.4±0.7

[a] Concentration of metal compound.
[b] Mean diameter of metal crystallites.
[c] Not determined.

intensity, stirring speed, volume of the suspension and temperature, that gave Au and Pt particles with a reasonable dispersion. For example, the FD of Au at 343 K, an optimum temperature for the DP method, led to the deposition of all Au within less than 20 min, but the size distribution of the Au particles shifted to diameters larger than 10 nm. The deposition parameters shown in Table 1 represent the best conditions that could be obtained in our system. The rates of Au and Pt deposition ranged from 2.5 to 5 μmol h^{-1}. These rates are in good agreement with the values reported in earlier studies [16,21–23]. For instance, Herrmann et al. [21] performed a detailed study of the photochemical deposition of Pt onto a suspension of 5 g dm^{-3} anatase using a variety of Pt complexes and a radiant intensity of 60 mW cm^{-2}. They reported a deposition rate of about 7.9 μmol Pt h^{-1} for H_2PtCl_6. In addition, a decrease in the pH of the suspensions was observed during the FD of Au and Pt. For example, the pH dropped from 4 to about 3.5 during the preparation of 1%Pt–TiO_2 and from 7.2 to about 4.6 in the case of 1.1%Au–TiO_2. This decline in pH can be attributed to the formation of H^+ ions from the photooxidation of water and methanol (see Eqs. (6) and (7) in Section 4.1) [21].

The data for the DP method are compiled in Table 2. Platinum deposition was carried out in the optimum pH range (pH 4–6.5) for the adsorption of $PtCl_6^{2-}$ on TiO_2, as shown elsewhere [19,20]. In the case of Au–TiO_2-DP, the loading and particle size of gold were controlled by varying the pH and concentration of $HAuCl_4$ (C_{HAuCl4}) in the starting suspensions [31]. For suspensions with the same C_{HAuCl4} value, an increase in the pH value led to an increase in the amount of deposited Au, reaching a maximum at pH 6, and decreasing at pH > 6. On the other hand, the size of the Au crystallites decreased consistently with increasing pH up to pH 9. The most probable explanation for these phenomena can be sought in the solution chemistry of gold precursors, i.e. the changing adsorption characteristics of Au complexes on TiO_2 grains. When TiO_2 is added to an aqueous solution containing gold complexes, the surface polarization results in a net electrical surface charge at the TiO_2–solution interface. The nature and magnitude of this charge are a function of, among other things, the pH of the suspension. In the pH range 4–6, the surface of TiO_2 is positively charged. This may lead to a strong interaction between TiO_2 and gold complexes, such as $AuOHCl_3^-$ or $Au(OH)_2Cl_2^-$, facilitating the adsorption of these anions on TiO_2 and consequently leading to a higher Au loading. On the other hand, at pH > 6, the isoelectric point for TiO_2 [19,44–46], TiO_2 particles carry a negative charge, thus reducing the electrostatic interaction with Au complexes in solution, which in this case are mainly $Au(OH)_3Cl^-$ [47], leading to a decrease in the overall amount of Au complex anions adsorbed on TiO_2 and the final Au content. This explanation is supported by previous studies which show that TiO_2 behaves as an

Table 2
Parameters for the deposition–precipitation (DP), physical mixing (MIX) and impregnation (IMP) methods of Au and Pt on TiO_2 (the volume of the metal compound solution containing TiO_2 powders ($HAuCl_4$–TiO_2, H_2PtCl_6–TiO_2) was 300 cm^3 for entries 1–8, 207 cm^3 for entries 12–14 and 20 cm^3 for entries 9 and 15)

Experiment/ suspension/method	m_{TiO2} (g)	Concentration [a] (mM)	pH [b]	Loading [c] (wt.%)	d [d] (nm)
$HAuCl_4$–TiO_2					
1 DP	1.6	0.95	10	0.4	2.5±0.5
2 DP	1.6	3.3	10	0.5	3.5±1.1
3 DP	1.6	3.3	9	1.8	2.7±0.6
4 DP	1.6	3.3	8.2	2.3	2.5±0.6
5 DP	1.6	3.3	8	2.2	3.2±0.7
6 DP	1.0	2.2	7	3.1	3.2±0.8
7 DP	1.0	2.2	6	4.5	4.2±0.8
8 DP	1.0	2.2	4	2.8	18.2±0.4
9 IMP	≈2	5.4	2	1.1	–
10 MIX-473 K [e]	5	–	–	3.0	5.1±1.3
11 MIX-873 K [e]	5	–	–	3.0	11.6±2.5
H_2PtCl_6–TiO_2					
12 DP	2.2	0.27	7	0.4	1.4±0.3
13 DP	2.2	0.53	6	1.0	2.0±0.9
14 DP	2.2	0.53	4.5	1.1	1.3±0.3
15 IMP	≈2	5.1	–	1.0	1.4±0.3

[a] Concentration of $HAuCl_4 \cdot 4H_2O$ or $H_2PtCl_6 \cdot 6H_2O$.
[b] pH of the suspension.
[c] Amount of Au or Pt deposited on TiO_2.
[d] Average diameter of the deposited metal particles was determined by measuring 100–600 particles on transmission electron micrographs for each sample. The amount of Cl^- in Au–TiO_2-DP was between 20 and 50 ppm and in Pt–TiO_2-DP was between 30 and 50 ppm.
[e] Samples prepared by physical mixing of colloidal gold with TiO_2.

anion exchanger in acidic and neutral solutions and a cation exchanger in basic solutions [19,44]. This phenomenon can also be ascribed to the influence of other functional groups or competing ions on the TiO_2 surface. For example, it was observed in earlier studies that, in some cases, protons or hydroxyl groups can fix metal complexes to the support surface [48,49]. The large mean diameters of Au crystallites obtained at low pH may indicate the chemisorption of Au complex anions at particular sites on the TiO_2 grains, followed by the adsorption of the anions near the same nuclei. An additional factor is the difference in mobility of the different Au precursors during calcination. As mentioned in Section 2.2.2, during repetitive washing of the obtained slurry, Cl^- ions are successively removed from the surface and the final Au precursor is mainly in the form of $Au(OH)_3$, which is converted to Au_2O_3 and eventually to metallic Au during drying and air calcination. The concentration of Cl^- in Au–TiO_2-DP samples was between 20 and 50 ppm.

3.2. Reaction products

Table 3 summarizes the reaction products obtained from the irradiation of an aqueous suspension containing 1wt.%Au–TiO_2-FD and 1wt.%Pt–TiO_2-FD in 30 cm^3 of 5 M C_2H_5OH. The main gaseous products were hydrogen, methane and carbon dioxide. The major liquid product was acetaldehyde. Small amounts of acetic acid were also produced. The types of product shown in Table 3 are in accordance with the results usually obtained from the irradiation of Pt–TiO_2 suspensions in aqueous solutions of primary alcohols [24,25,42,43]. A more detailed overall mass balance of the reaction products will be studied and published elsewhere. In the following sections, the photocatalytic activities of Au–TiO_2 and Pt–TiO_2 are compared on the basis of the yields and rates of hydrogen production, since H_2 is the main, direct product of the reaction, and its

Table 3
Reaction products from aqueous suspensions containing TiO_2-FD, 1wt.%Au–TiO_2-FD and 1wt.%Pt–TiO_2-FD in 5 M C_2H_5OH under argon (catalyst, 1.7 g dm^{-3}; reaction temperature, 310 K; pH 4–5; suspension was irradiated for 10 h with a 500 W Hg lamp operated at 30 mW cm^{-2})

Product type	Product yield (mmol)		
	TiO_2-FD	1%Au–TiO_2-FD	1%Pt–TiO_2-FD
H_2	0.07	2.07	3.08
CH_4	n.d. [a]	0.04	0.09
CO_2	Trace	0.03	0.09
CH_3CHO	0.08	1.43	1.64
CH_3COOH	n.d.	Trace	Trace

[a] Not detected.

concentration can be accurately and easily followed during the irradiation experiments.

3.3. Photocatalytic activity

3.3.1. Activity of photodeposited samples

Fig. 4(a) illustrates the activity of Au and Pt catalyst samples prepared by photochemical deposition. Only slight differences were observed between the activities of unsupported TiO_2-DP, TiO_2-FD, TiO_2-IMP and TiO_2-MIX. These materials exhibited a poor activity towards the formation of H_2. The deposition of Au or Pt on TiO_2 resulted in a substantial improvement in the H_2 yield. The yield obtained in the case of Pt–TiO_2-FD is of the same order of magnitude as that observed by Sakata and Kawai [43] who obtained about 4–5 mmol H_2 from 10 g dm^{-3} Pt(4%)–TiO_2 suspended in 50% ethanol solution after 10 h of irradiation. As illustrated in Fig. 4(a), the amount of H_2 produced over both catalysts increased almost linearly with illumination time in the first 3 h, followed by a gradual decrease in the production rate for longer illumination periods. In photocatalytic batch systems, long illumination periods usually result in a progressive decline in the rate of H_2 generation (as observed here) due, in part, to back reactions as products start to build up in the reaction system, deactivation of the photocatalyst and/or pressure buildup in the gas phase; this has been demonstrated previously [19,25,41a,50–52].

A comparison of the activity of Au–TiO_2-FD and Pt–TiO_2-FD shows that the activity of Au samples is about 30% lower than that of Pt samples; this is a modest value considering that for a long time gold has been regarded as catalytically far less active than Pt in photochemical processes. In an early paper, Hussein and Rudham [28] reported that Au–TiO_2 exhibited no activity for the photochemical dehydrogenation of propan-2-ol. Kanno et al. [37] conducted a study on H_2 production from methanol solutions over a variety of catalysts in which TiO_2 was prepared from titanium isopropoxide. They reported that the activity of Pt–TiO_2 was approximately three times higher than that of Au–TiO_2. It seems that such discrepancies stem from differences in catalyst preparation and pretreatment methods. Recent studies using small, highly dispersed gold particles deposited on a variety of supports have shown that gold catalysts are very active, e.g. in the low temperature oxidation of carbon monoxide [31,32,34,53–58], the hydrogenation of CO_2 [33,59], the oxidation of organic compounds in wastewater [60] and the hydrogenation of alkenes [61]. In these studies, the preparation and pretreatment procedures and the dispersion of gold particles affected the activity of the catalysts.

Fig. 4(b) depicts the amount of CH_4 and CO_2 produced concomitantly with H_2 as a function of the illumination time. In contrast with H_2 evolution, an initial induction period of 1–2 h was observed for CH_4 and CO_2, followed by a gradual growth with time. This period was about 0.7 h (CH_4) and 1 h (CO_2) for Pt–TiO_2-FD and 1.5 h (CH_4) and 2 h (CO_2) for Au–TiO_2-FD. The differences in the evolution periods observed between Au and Pt samples may indicate that these products are secondary

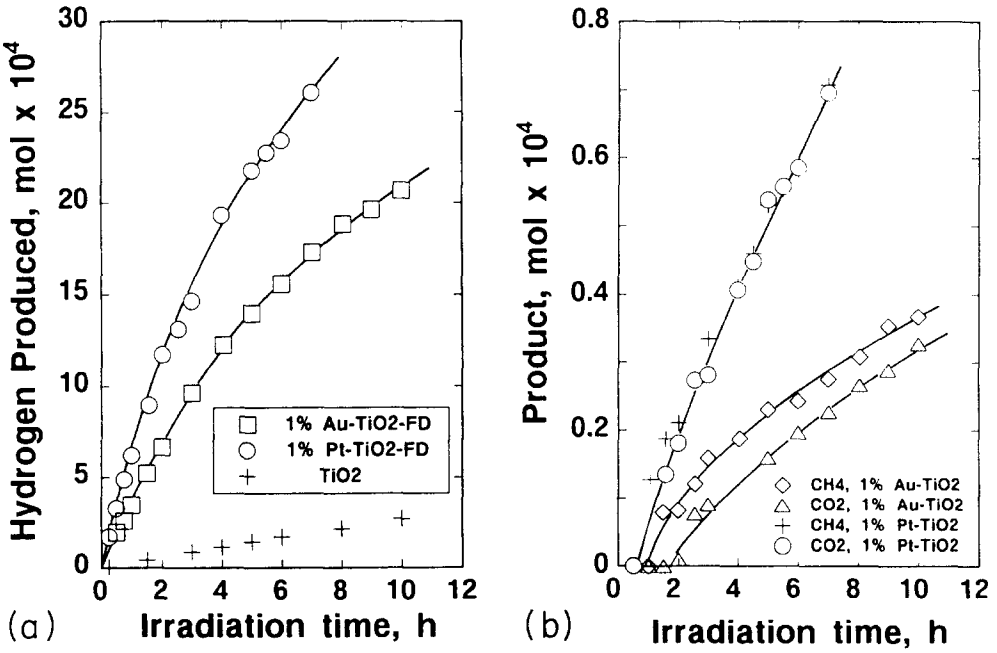

Fig. 4. (a) Activity of 1wt.%Au–TiO_2-FD and 1wt.%Pt–TiO_2-FD for H_2 production from an aqueous suspension containing 5 M C_2H_5OH. Catalyst, 1.7 g dm^{-3}; reaction temperature, 310 K; initial pH 4–5; light intensity, 30 mW cm^{-2}. (b) Time course of CH_4 and CO_2 production. Experimental conditions and catalysts are the same as in (a).

in nature, i.e. intermediate species from which CH_4 and CO_2 are produced must be formed before the appearance of these products in the gas phase (see later). It is also interesting to consider the relation between the gas phase products. The H_2/CH_4 ratios were about 35 and 50 for Pt and Au samples, as can be seen in Table 3 and Figs. 4(a) and 4(b). At the same time, the H_2/CO_2 ratios were about 35 and 70 for Pt and Au samples respectively. Furthermore, an inspection of Fig. 4(b) reveals that the CH_4/CO_2 ratio over Pt–TiO_2-FD tends to unity with irradiation time, whereas for Au–TiO_2-FD this ratio is consistently higher than unity. On the basis of this result, we may speculate that the observed differences originate from the hydrogenation of CO_2 (a photocatalytic reaction that has been observed in aqueous suspensions of $SrTiO_3$ [62], Ru–RuO_x–TiO_2 [63], Ru–TiO_2 [64] and Cu–TiO_2 [65]) and that this reaction is favoured over Au–TiO_2-FD. Variation of the CO_2/CH_4 ratio can be attributed to two competing reactions, as will be shown later in the text (see Eqs. (16) and (17), Section 4.2). Another notable feature of the above results is that Pt deposits give a slightly higher long-term activity than Au, as observed in Figs. 4(a) and 4(b).

3.3.2. *Activity of DP, IMP and MIX samples*

The production of H_2 over various DP, IMP and MIX samples is compared in Fig. 5 and Table 4. Similar trends in H_2 production behaviour were observed as in the FD samples in Fig. 4(a). It can also be seen that, although the curves for Au and Pt catalysts are very close initially, they tend to separate at longer illumination times. The activity of Au–TiO_2-MIX was similar to that of Au–TiO_2-IMP, indicating that a strong interaction between Au and TiO_2 is necessary to obtain appreciable H_2 yields. As shown in Fig. 5 and Table 4, Au–TiO_2-DP displayed a better catalytic activity than Au–TiO_2-IMP or Au–TiO_2-MIX samples. The differences between Pt–TiO_2-IMP and Pt–TiO_2-DP were less pronounced than those observed for the Au samples. The ratios $H_{2,Pt\text{–}TiO2\text{-}DP}/H_{2,Au\text{–}TiO2\text{-}DP}$, H_2/CH_4 and H_2/CO_2 and the induction periods were similar to those observed in FD samples. From a comparison of the H_2 yields in Figs. 4(a) and 5 and Table 4, it is noted that, for catalysts with a similar metal content, FD samples display a higher activity than DP samples. A possible explanation for this difference in activity is that, during photochemical deposition, the deposition of gold and platinum particles occurs at or near the site of photoexcitation. This, in turn, may facilitate the efficient transport of photogenerated electrons from TiO_2 to the metal particles during H_2 production experiments.

3.3.3. *Influence of pretreatment conditions*

To explore the influence of pretreatment on the catalytic activity, a series of runs was conducted on catalysts that were calcined and reduced for various periods and temperatures. The activities of a variety of DP catalysts, prepared under various pretreatment conditions, are illustrated in Table 5. The reduction

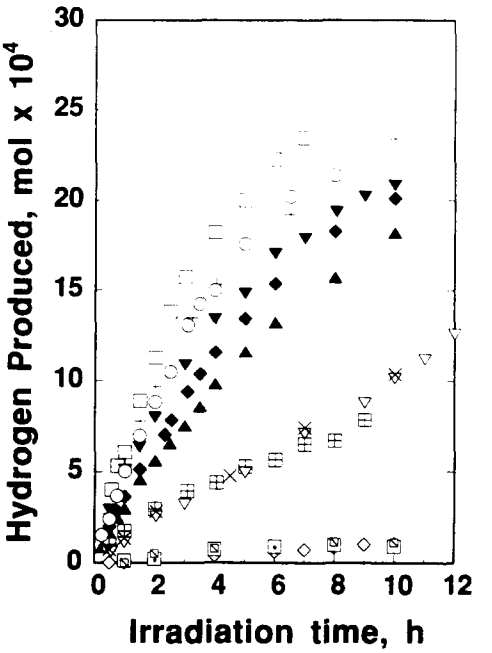

Fig. 5. Comparison between the H_2 evolution of Au and Pt samples vs. the illumination time for catalysts prepared by deposition–precipitation (DP), impregnation (IMP) and by mixing TiO_2 with Au colloids (MIX): □, 0.5%Pt–TiO_2-DP; +, 0.9%Pt–TiO_2-DP; ⊙, 1%Pt–TiO_2-IMP; ▲, 0.34%Au–TiO_2-DP; ▼, 1.8%Au–TiO_2-DP; ◆, 2.2%Au–TiO_2-DP; ⊞, 1.1%Au–TiO_2-IMP; ▽, 3%Au–TiO_2-MIX calcined at 473 K; ×, 3%Au–TiO_2-MIX calcined at 873 K; ⧅, TiO_2-DP; ◇, TiO_2-IMP; ⊡, TiO_2-MIX-473 K. Conditions are the same as in Fig. 4(a).

Table 4
Turnover rates of hydrogen production for various catalysts. Hydrogen generation conditions: suspension, 1.7 g dm^{-3}; temperature, 310 K; pH_0, 4.5–5; incident flux, 30 mW cm^{-2}

Catalyst	H_2 turnover rate * (μmol g min^{-1} m^{-2})
0.34%Au–TiO_2-DP	7.47
1.8%Au–TiO_2-DP	2.56
2.2%Au–TiO_2-DP	1.90
3.2%Au–TiO_2-DP	1.30
1.0%Au–TiO_2-FD	7.81
3%Au–TiO_2-MIX-473 K	0.84
0.4%Pt–TiO_2-DP	8.94
1.0%Pt–TiO_2-DP	3.70
1.0%Pt–TiO_2-IMP	3.53
0.9%Pt–TiO_2-FD	8.85

* The yields of H_2 production used for calculating the turnover rates were obtained by subtracting the yields of the reference blanks without metal, i.e. unsupported TiO_2-DP, TiO_2-FD, TiO_2-IMP and TiO_2-MIX, from the total yields obtained from catalysts with the supported metal, i.e. metal–TiO_2. The total surface areas of gold and platinum were calculated by assuming hemispherical metal clusters.

Table 5
Effect of pretreatment conditions on the H_2 yield after 3 h of irradiation. All samples were prepared by DP. Hydrogen generation conditions: suspension, 1.7 g dm^{-3}; temperature, 310 K; pH_0, 4.5–5; incident flux, 30 mW cm^{-2}

Experiment	Sample	$T_{air,calc.}$ [a] (K)	$t_{reduction}$ [b] (h)	H_2 yield/3 h (mol×10^4)
1	0.4%Au–TiO_2	673	10	7.51
2	0.34%Au–TiO_2	673	10	7.62
3	0.5%Au–TiO_2	573	10	7.87
4	0.5%Au–TiO_2	673	10	7.77
5	0.5%Au–TiO_2	773	10	5.91
6	2.2%Au–TiO_2	673	10	9.15
7	3.2%Au–TiO_2	673	10	8.17
8	0.4%Pt–TiO_2	673	10	15.72
9	1.0%Pt–TiO_2	573	10	14.79
10	1.0%Pt–TiO_2	673	10	13.19
11	1.0%Pt–TiO_2	773	10	11.72
12	1.0%Pt–TiO_2	673	7	11.74
13	1.0%Pt–TiO_2	673	20	13.15
14	1.0%Pt–TiO_2, recalculated [c]	673	20	13.56

[a] Samples were first calcined in air at temperatures $T_{air,calc.}$ for 4 h.

[b] $t_{reduction}$ denotes the H_2 reduction time (1 vol.% H_2 in N_2 at 723 K).

[c] Reduced sample in experiment 13 was calcined again in air at 673 K for 4 h.

temperature in the range 673–773 K had little effect on the activity of both Au and Pt samples, and so was fixed at 723 K [66]. In addition, only a slight variation of the activity was observed with the reduction time as shown in Table 5. Thus, in further experiments, the catalyst samples were reduced for 10 h. For both Au and Pt samples, the yield of H_2 (n_H) was affected by the air calcination temperature and followed the sequence $n_{H,573\,K} > n_{H,673\,K} > n_{H,773\,K}$. This trend is similar to that found previously in the system Au–TiO_2-DP–ethylene glycol [41a] and that reported previously for Pt–TiO_2 [37]. Although X-ray diffraction measurements did not show any significant changes in the crystallinity of the catalysts calcined at various temperatures, this decline in activity with air calcination temperature can be ascribed to structural and chemical changes taking place in TiO_2. The transition of the TiO_2 support from anatase to the more thermodynamically stable rutile at calcination temperatures higher than 673 K has been pointed out by several workers [15,67]. Also, the superior activity of anatase compared with rutile has been previously observed in a number of photocatalytic reactions [15,28,68,69]. Thus it is reasonable to assume that the observed reduction in activity for samples calcined at temperatures higher than 673 K is due, in part, to the changes in surface crystallinity of TiO_2, i.e. to the rise in the proportion of rutile on the surface of our catalysts. In another experiment, in order to check whether the reduced state of TiO_2, because of the treatment in H_2, has any effect on the photoactivity, pre-reduced Pt–TiO_2 samples were calcined again in air at 673 K for 4 h. As shown by entries 13 and 14 in Table 5, no significant change in activity was observed.

3.4. Influence of the metal content

Typical representations of H_2 evolution as a function of time for FD samples with various Au and Pt loadings are shown in Figs. 6 and 7 respectively. The activity towards H_2 production increased with increasing metal content up to about 1–2 wt.% Au and 0.3–1 wt.% Pt and then decreased thereafter. A similar trend was observed in Fig. 5 for Au–TiO_2-DP. This trend in catalytic behaviour is consistent with previously measured H_2 production vs. Au loading from the Au–TiO_2-DP–ethylene glycol system [41a]. It is worth noting that air calcination of 1.2%Au–TiO_2-FD at 400 °C did not result in a change in its activity (see Fig. 6). This result indicates that almost all gold precursors on TiO_2 grains have been reduced to metallic gold during FD.

Detailed studies of the influence of metal loading on H_2 production have been conducted previously on a series of Pt–TiO_2 catalysts [19,25,48,70]. It was found that the H_2 yield increased initially with increasing Pt content of the catalyst, reached a maximum and then started to decrease once the Pt content was increased beyond a certain point, usually 0.5–1%. The reason given for this trend in reaction behaviour is that the deposition of small amounts of Pt is indispensable for the removal of photogenerated electrons from TiO_2,

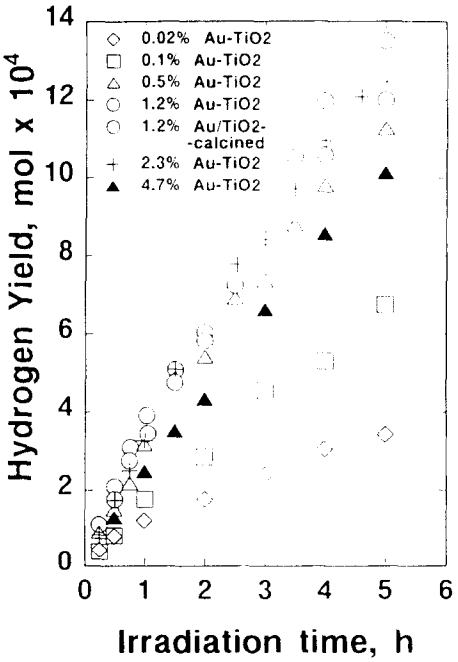

Fig. 6. Effect of Au content on the H_2 yield. Conditions are the same as in Fig. 4(a).

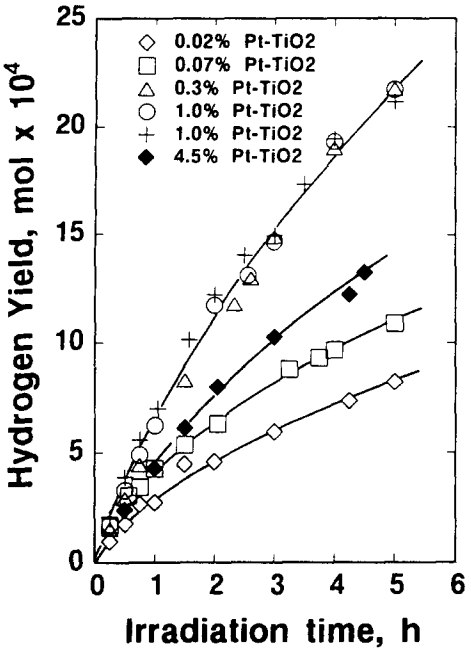

Fig. 7. Influence of Pt loading on the H_2 yield. Other parameters are the same as in Fig. 4(a).

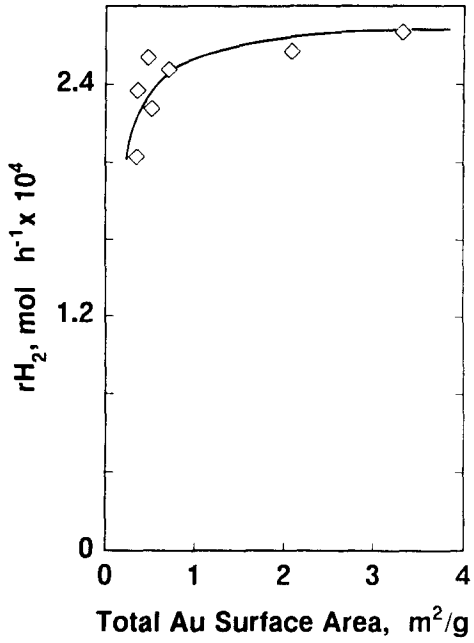

Fig. 8. Rate of H_2 production as a function of the total exposed Au surface area. The total surface area of Au was calculated by assuming hemispherical metal clusters.

their storage and for the reduction reaction. However, as more and more Pt is added to the TiO_2 surface beyond a certain optimal value, blockage of the photosensitive TiO_2 surface occurs, thus decreasing the surface concentration of electrons and holes available for reaction. Hence after this optimal point, the H_2 yield starts to decrease. Another explanation is that, at higher metal loadings, the deposited metal particles may act as recombination centres for photogenerated electrons and holes [26,71]. Similar reasons can be given to explain the effects of the metal content observed in Figs. 6 and 7. One of the probable reasons for the appearance of a maximum H_2 yield at a relatively high metal loading of 1–2 wt.% Au is that the mean particle diameter for Au is larger than that of Pt, and thus a slightly higher Au loading is required to give the same number of particles.

3.5. Dependence on the surface area of gold

The effect of the gold surface area on the rate of hydrogen evolution was investigated using DP samples with various gold particle diameters. The total exposed surface area of gold was calculated from the Au content and the mean diameter of the gold particles, assuming that the gold crystallites are hemispherical, as shown in Fig. 3. For the purpose of obtaining reliable data, the mean rates of H_2 production were measured in the illumination time range 1–6 h. The rates were approximately constant during this period of time, as illustrated in Fig. 5. Fig. 8 shows the relationship between the rate of H_2 formation and the exposed surface area of gold. As reported previously [41a], the rate of H_2 production increased slightly with the surface area of deposited Au particles. A similar weak dependence of the rate of H_2 evolution on the geometrical factors of metal particles has been observed for photocatalysts containing platinum [25,48]. Therefore we can conclude that the activity of Au–TiO_2 towards H_2 production is not directly associated with the exposed surface area of gold. This is not surprising since recent studies indicate that the essential reaction steps in photocatalytic processes occur on the semiconductor surface [4,28,72]. Also, as pointed out by the referee, in addition to the main role played by the metal surface in photocatalytic systems, there is a possibility of the participation of sites located at the microinterfaces between Au or Pt particles and TiO_2 as locations for the photoredox effects. No attempt was made to determine the effect of the surface area of Pt, because the mean diameters of the Pt particles did not vary substantially with the Pt loadings for the samples used in our experiments.

3.6. Effect of pH

The initial pH of the suspension was adjusted to the desired level by the addition of appropriate quantities of either NaOH or H_2SO_4. The hydrogen production as a function of irradiation time at various pH values for 2.2%Au–TiO_2-DP suspensions is presented in Fig. 9. As can be seen, the amount of H_2 evolved was strongly dependent on the initial pH. pH values in the range 4–7 gave better H_2 yields, whereas highly acidic

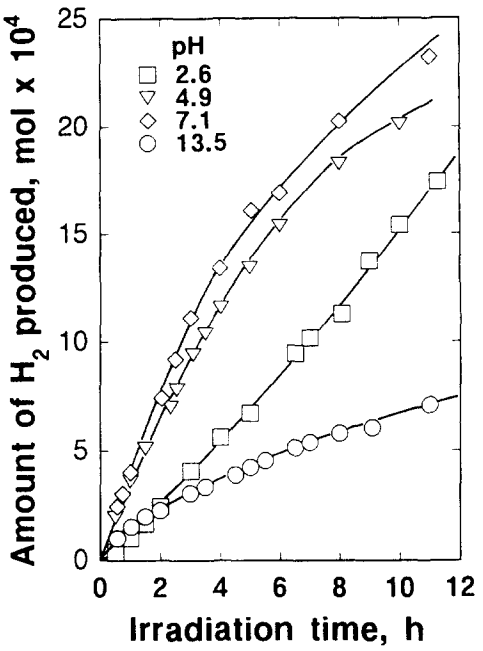

Fig. 9. Hydrogen production as a function of irradiation time for suspensions of 2.3wt.%Au–TiO_2-DP in 5 M C_2H_5OH at various pH values.

and basic suspensions resulted in a considerable decrease in the H_2 yield. Another noticeable observation was that the final pH of the suspensions was generally lower than the values before irradiation. For example, the pH dropped from about 7.1 before illumination to 4.7 after 10 h of irradiation. These results correlate well with observations reported in the literature. Sakata and Kawai [43], who studied H_2 generation from a variety of organic compounds, reported the decline of H_2 production from Pt–TiO_2–C_2H_5OH suspensions with increasing OH^- concentration. Miyake et al. [42] reported that significant photo-oxidation of methanol and 2-propanol on TiO_2 takes place only at pH 7–8. More work will be necessary to establish unambiguously the reason for the pH phenomenon.

4. Discussion

4.1. Mechanism of deposition of Au and Pt

As described earlier, the deposition of gold or platinum by DP or FD is initiated by the electrostatic interaction between the TiO_2 particles and metal complex species in solution, such as $AuCl_4^-$, $AuOHCl_3^-$, $Au(OH)_2Cl^-$, $Au(OH)_3Cl^-$ or $PtCl_6^{2-}$, providing a discrete concentration of adsorbed metal precursors on TiO_2. According to the results discussed above, the amount and type of adsorbed metal precursor depend on several parameters, such as the initial concentration of $AuCl_4^-$ and $PtCl_6^{2-}$, the concentration of TiO_2, the pH and temperature.

In the case of DP and IMP, the adsorbed precursors are reduced to metallic particles by air calcination and reduction in an H_2 atmosphere, forming small, well-dispersed particles. In FD, the reaction is initiated when light energy larger than the TiO_2 band gap ($E_{BG,TiO2}$ = 3.23 eV [73]) is absorbed by the TiO_2 particles, forming an electron (e^-) and hole (h^+) pair in the semiconductor as described in Eq. (1). The recombination of electron and holes in the lattice can be avoided if the two species are separated and subsequently trapped by appropriate sites or transferred to species bound to the surface, as illustrated in Eqs. (2) and (3)

$$(TiO_2) + h\nu \longrightarrow e_{CB}^- + h_{VB}^+ \quad (1)$$

$$e_{CB}^- \longrightarrow e_{tr}^- \quad (2)$$

$$h_{VB}^+ \longrightarrow h_{tr}^+ \quad (3)$$

The subscripts CB and VB denote the conduction and valence bands respectively. The subscript tr denotes a trap. The reduction processes involve the reduction of metal complexes to metallic Au and Pt (Eqs. (4) and (5))

$$AuCl_4^- + 3e_{tr}^- \longrightarrow Au + 4Cl^- \quad (4)$$

$$PtCl_6^{2-} + 4e_{tr}^- \longrightarrow Pt + 6Cl^- \quad (5)$$

The oxidation processes involve the oxidation of H_2O or CH_3OH by the trapped hole from Eq. (3)

$$h_{tr}^+ + H_2O \longrightarrow H^+ + {}^{\bullet}OH \quad (6)$$

$$2h_{tr}^+ + CH_3OH \longrightarrow 2H^+ + HCHO \quad (7)$$

In addition to the parameters given above, the final Au and Pt loadings obtained during FD depend on the gas phase medium, the type and concentration of hole scavengers and the illumination time and intensity [20–23].

4.2. Mechanism of hydrogen evolution

In the case of hydrogen production experiments, the reduction process involves the reduction of protons by electrons trapped on metal sites (e_{tr}^-(Me)), leading to the production of H_2 according to the following equations

$$e_{tr}^-(Me) + H_{sol}^+ \longrightarrow H_{ads}({}^{\bullet}H) \quad (8)$$

$$2H_{ads} \longrightarrow H_{2,\,ads} \quad (9)$$

$$H_{2,\,ads} \longrightarrow H_{2,\,sol} \quad (10)$$

$$H_{2,\,sol} \longrightarrow H_{2,\,gas} \quad (11)$$

where the subscripts sol and ads denote the solution phase and the adsorbed state respectively. Surface trapped holes will interact with water (see Eq. (6)) or adsorbed C_2H_5OH producing protons and acetaldehyde

according to the mechanism suggested by Sakata and Kawai [43]

$$2h_{tr}^{+} + C_2H_5OH \longrightarrow 2H^{+} + CH_3CHO \quad (12)$$

$$2h_{tr}^{+} + CH_3CHO + H_2O \longrightarrow 2H^{+} + CH_3COOH \quad (13)$$

Methane and CO_2 are produced by the decomposition of acetic acid from Eq. (13) according to the photo-Kolbe decarboxylate route [15]

$$h_{tr}^{+} + CH_3COO^{-} \longrightarrow CO_2 + CH_3^{\cdot} \quad (14)$$

Another possible pathway for CH_4 formation may be the hydrogenation of CO_2 according to

$$CO_2 + 4H_2 \xrightarrow[\text{photocatalyst}]{h\nu} CH_4 + H_2O \quad (15)$$

The overall reaction mechanism for the production of H_2 from aqueous C_2H_5OH can be summarized as two competing reactions as shown in Eqs. (16) and (17) [74]

$$C_2H_5OH + H_2O \xrightarrow[\text{photocatalyst}]{h\nu} 2H_2 + CH_4 + CO_2 \quad (16)$$

$$C_2H_5OH + 3H_2O \xrightarrow[\text{photocatalyst}]{h\nu} 2CO_2 + 2H_2 \quad (17)$$

Another possible reaction pathway is the involvement of adsorbed surface hydroxyls on TiO_2 in the trapping of holes [72,75,76]. The interaction of surface hydroxyl groups with holes will result in the formation of hydroxyl radicals which, in turn, will interact with C_2H_5OH or its intermediates adsorbed on the metal–TiO_2 surface or present in the vicinity to produce CO_2 and other minor products.

5. Conclusions

This study shows that it is possible to prepare Au–TiO_2 samples of reasonable activity for the production of hydrogen from aqueous suspensions. The deposition of Au and Pt was carried out using TiO_2 powder in aqueous suspensions containing $HAuCl_4 \cdot 4H_2O$ or $H_2PtCl_6 \cdot 6H_2O$ by photochemical deposition, deposition–precipitation, impregnation and, in the case of Au, by mixing TiO_2 with gold suspensions. Our principal findings and conclusions are as follows.

(1) The activity of Au catalysts for H_2 production strongly depends on the method of preparation and decreases in the order Au–TiO_2-FD > Au–TiO_2-DP > Au–TiO_2-IM P > Au–TiO_2-MIX. The activity of platinum samples is less sensitive to the preparation method and decreases in the order Pt–TiO_2-FD > Pt–TiO_2-DP ≈ Pt–TiO_2-IM P.

(2) The yield of H_2 depends on the pretreatment conditions. Gold and platinum precursors calcined in air at 573 K have the highest activity towards H_2 generation, followed by a decline in activity with increasing calcination temperature.

(3) The maximum H_2 yield is observed for Pt and Au loadings of 0.3–1 wt.% and 1–2 wt.% respectively. The exposed surface area of gold has only a small influence on the rate of hydrogen generation.

(4) The rate of H_2 production strongly depends on the initial pH of the suspension. pH values in the range 4–7 give better H_2 yields, whereas highly acidic and basic suspensions result in a considerable decrease in the H_2 yield.

(5) The roles of Au and Pt on TiO_2 seem to involve the attraction and trapping of photogenerated electrons, the reduction of protons and the formation and desorption of hydrogen. The higher overall activity of Pt samples is probably a result of the more effective trapping and pooling of photogenerated electrons by Pt and/or because platinum sites have a higher capability for the reduction reaction.

Acknowledgements

G.R.B. gratefully acknowledges the financial support of the Science and Technology Agency of Japan. The comments of Professor Hisashi Harada on the manuscript are gratefully acknowledged. We are indebted to Mrs. Toshiko Nakamura for her assistance in the literature search and for performing the particle size analysis.

References

[1] J.M. Herrmann, J. Disdier, M.N. Mozzanenga and P. Pichat, *J. Catal., 60* (1979) 369.
[2] G. Hodes and M. Graetzel, *Nouv. J. Chim., 8* (1984) 509.
[3] E. Pelizzeti and N. Serpone, *Homogeneous and Heterogeneous Photocatalysis*, NATO ASI Series, Reidel, Dordrecht, 1986, and references cited therein.
[4] M. Anpo, *Res. Chem. Intermed., 11* (1989) 67.
[5] (a) A.J. Bard, *J. Photochem., 10* (1979) 59. (b) A.J. Bard, *Science, 207* (1980) 139.
[6] (a) S.N. Frank and A.J. Bard, *J. Chem. Soc., 99* (1977) 4667. (b) S.N. Frank and A.J. Bard, *J. Phys. Chem., 81* (1977) 1484.
[7] I. Izumi, W.W. Dunn, K.O. Wibourn, F.R. Fan and A.J. Bard, *J. Phys. Chem., 84* (1980) 3207.
[8] J.H. Carey, J. Lawrance and H.M. Tosine, *Bull. Environ. Contam. Toxicol., 16* (1986) 697.
[9] M.A. Fox and C.C. Chen, *J. Am. Chem. Soc., 103* (1981) 6757.
[10] C.Y. Hsiao, C.L. Lee and D.F. Ollis, *J. Catal., 82* (1983) 628.
[11] (a) R.W. Matthews, *J. Catal., 97* (1986) 565. (b) R.W. Matthews, *J. Phys. Chem., 91* (1987) 3328. (c) R.W. Matthews, *Water Res., 24* (1990) 563.
[12] M. Schiavello, *Photocatalysis and Environment, Trends and Applications*, NATO ASI Series, Vol. 237, Kluwer, Dordrecht, 1988.
[13] A. Fujishima and K. Honda, *Nature, 238* (1972) 37.
[14] (a) M. Graetzel, *Energy Resources Through Photochemistry and Catalysis*, Academic Press, New York, 1983. (b) E. Pelizzetti and M. Schiavello, *Photochemical Conversion and Storage of Solar Energy*, Kluwer, Dordrecht, 1990.

[15] B. Kraeutler and A.J. Bard, *J. Am. Chem. Soc., 100* (1978) 5985.
[16] (a) W.W. Dunn and A.J. Bard, *Nouv. J. Chim., 5* (1981) 651. (b) H. Reiche, W.W. Dunn and A.J. Bard, *J. Phys. Chem., 83* (1979) 2248.
[17] H. Yoneyama, N. Nishimura and H. Tamura, *J. Phys. Chem., 85* (1981) 268.
[18] S. Teratani, J. Nakamichi, K. Taya and K. Tanaka, *Bull. Chem. Soc. Jpn., 55* (1982) 1688.
[19] J. Kiwi and M. Graetzel, *J. Phys. Chem., 88* (1984) 1302.
[20] J.S. Curran, J. Domenech, N. Jaffrezic-Renault and R. Philippe, *J. Phys. Chem., 89* (1985) 957.
[21] J.M. Herrmann, J. Disdier and P. Pichat, *J. Phys. Chem., 90* (1986) 6028.
[22] E. Borgarello, R. Harris and N. Serpone, *Nouv. J. Chim., 9* (1985) 743.
[23] E. Borgarello, N. Serpone, G. Emo, R. Harris, E. Pelizzetti and C. Minero, *Inorg. Chem., 25* (1986) 4499.
[24] T. Kawai and T. Sakata, *J. Chem. Soc., Chem. Commun.*, (1980) 694.
[25] P. Pichat, M.N. Mozzanega, J. Disdier and J.M. Herrmann, *Nouv. J. Chim., 6* (1982) 559.
[26] H. Courbon, J.M. Herrmann and P. Pichat, *J. Phys. Chem., 88* (1984) 5210.
[27] I.A. Ichou, M. Formenti and S.J. Teichner, in S. Kaliaguine and A. Mahay (eds.), *Catalysis in Energy Scene*, Elsevier, Amsterdam, 1984, p. 297.
[28] F.H. Hussein and R. Rudham, *J. Chem. Soc., Faraday Trans. 1, 80* (1984) 2817.
[29] N.J. Renault, P. Pichat, A. Foissy and R. Mercier, *J. Phys. Chem., 90* (1986) 2733.
[30] M. Anpo, K. Chiba, M. Tomonari, S. Caluccia, M. Che and M.A. Fox, *Bull. Chem. Soc. Jpn., 64* (1991) 543.
[31] S. Tsubota, M. Haruta, T. Kobayashi, A. Ueda and Y. Nakahara, in G. Poncelet, P.A. Jacobs, P. Grange and B. Delmon (eds.), *Preparation of Catalysts*, Vol. 5, Elsevier, Amsterdam, 1991, p. 695.
[32] D. Cunningham, S. Tsubota, N. Kamijo and M. Haruta, *Res. Chem. Intermed., 19* (1993) 1.
[33] H. Sakurai, S. Tsubota and M. Haruta, *Appl. Catal., 102* (1993) 125.
[34] M. Haruta, S. Tsubota, T. Kobayashi, H. Kageyama, M.J. Genet and B. Delmon, *J. Catal., 144* (1993) 175.
[35] S.D. Lin and M.A. Vannice, *Catal. Lett., 10* (1991) 47.
[36] S.D. Lin, M. Bollinger and M.A. Vannice, *Catal. Lett., 17* (1993) 245.
[37] H. Kanno, Y. Yamamoto and H. Harada, *Chem. Phys. Lett., 121* (1985) 245.
[38] Y.M. Gao, W. Lee, R. Trehan, R. Kershaw, K. Dwight and A. Wold, *Mater. Res. Bull., 26* (1991) 1247.
[39] M. Albert, Y.M. Gao, D. Toft, K. Dwight and A. Wold, *Mater. Res. Bull., 27* (1992) 961.
[40] A. Harriman, *Platinum Metals Rev., 35* (1991) 22.
[41] (a) G.R. Bamwenda, S. Tsubota, T. Kobayashi and M. Haruta, *J. Photochem. Photobiol. A: Chem., 77* (1994) 59. (b) G.R. Bamwenda, S. Tsubota and M. Haruta, *Chem. Lett.*, submitted for publication.
[42] (a) M. Miyake, H. Yoneyama and H. Tamura, *Bull. Chem. Soc. Jpn., 50* (1977) 1492. (b) M. Miyake, H. Yoneyama and H. Tamura, *J. Catal., 58* (1979) 263.
[43] (a) T. Sakata and T. Kawai, *Nouv. J. Chim., 5* (1981) 279; *Chem. Phys. Lett., 80* (1981) 2. (b) T. Sakata and T. Kawai, *J. Photochem., 29* (1985) 205.
[44] (a) A.P. Boehm and M. Herrmann, *Z. Anorg. Chem., 352* (1967) 156. (b) A.P. Boehm and M. Herrmann, *Discuss. Faraday Soc., 352* (1971) 264.
[45] E.A. Barringer and H.K. Bowen, *Langmuir, 1* (1985) 420.
[46] (a) P.G. Johansen and A.S. Buchanan, *Aust. J. Chem., 10* (1957) 398. (b) G.A. Parks, *Chem. Rev., 65* (1965) 177.
[47] (a) H.L. Johnston and H.L. Leland, *J. Am. Chem. Soc., 60* (1938) 1439. (b) C.F. Baes and R.E. Mesmer, *The Hydrolysis of Cations*, E. Robert Klieger, Malabar, FL, 1986, p. 280.
[48] J.P. Brunelle, *Pure Appl. Chem., 50* (1978) 1211.
[49] G.D. Parfitt, *Pure Appl. Chem., 48* (1976) 415.
[50] K.E. Karakitsou and X.E. Verykios, *J. Catal., 134* (1992) 629.
[51] K. Sayama and H. Arakawa, *Shokubai (Catalyst), Catalysis Soc. Jpn., 35* (1993) 356.
[52] M. Schiavello, *Photoelectrochemistry, Photocatalysis and Photoreactors. Fundamentals and Developments*, Reidel, Dordrecht, 1985.
[53] J.D. Yates, *J. Colloid Interface Sci., 29* (1969) 194.
[54] M. Haruta, N. Yamada, T. Kobayashi and S. Iijima, *J. Catal., 115* (1989) 301.
[55] S.D. Gardner, G.B. Hoflund, B.T. Upchurch, D.R. Schryer, E.J. Kielinand and J. Schryer, *J. Catal., 129* (1991) 114.
[56] A. Knell, P. Barnickel, A. Baiker and A. Wokaun, *J. Catal., 129* (1992) 306.
[57] S.K. Tanielyan and R.L. Augustine, *Appl. Catal., 85* (1992) 73.
[58] C. Sze, E. Gulari and B.G. Demczyk, in S. Komarneni, J.C. Parker and G.J. Thomas (eds.), *Nanophase and Nanocomposite Materials, Mater. Res. Soc. Symp. Proc., 286* (1993) 143.
[59] S. Schild and A. Wokaun, *J. Chem. Soc., Faraday Trans., 87* (1991) 2821.
[60] K. Mitsui, T. Ishii, Y. Yamaguchi and K. Sano, Patent, Jpn. Kokai Tokkyo Koho Jpn. 04100595, 1992.
[61] G.C. Bond and P.A. Sermon, *Gold Bull., 6* (1973) 102.
[62] J.R. Hemminger, R. Carr and G.A. Somorjai, *Chem. Phys. Lett., 57* (1978) 100.
[63] K.R. Thampi, J. Kiwi and M. Graetzel, *Nature, 327* (1987) 506.
[64] M.R. Praire, A. Renken, J.G. Highfield, K.R. Thampi and M. Graetzel, *J. Catal., 129* (1991) 130.
[65] K. Hirano, K. Inoue and T. Yatsu, *J. Photochem. Photobiol. A: Chem., 64* (1992) 255.
[66] M.F.L. Johnson and C.D. Keith, *J. Phys. Chem., 67* (1963) 200.
[67] G. Sankar, K.R. Kannan and C.N.R. Rao, *Catal. Lett., 8* (1991) 27.
[68] R.B. Cundal, R. Rundham and M. Salim, *J. Chem. Soc., Faraday Trans. 1, 72* (1976) 1642.
[69] S. Nishimoto, B. Ohtani, H. Kajirawa and T. Kagiya, *J. Chem. Soc., Faraday Trans. 1, 81* (1985) 61.
[70] K. Domen, Y. Sakata, A. Kudo, K. Maruya and T. Onishi, *Bull. Chem. Soc. Jpn., 61* (1988) 359.
[71] J. Disdier, J.M. Herrmann and P. Pichat, *J. Chem. Soc., Faraday Trans. 1, 79* (1983) 651.
[72] C.S. Turchi and D.F. Ollis, *J. Catal., 122* (1990) 178.
[73] V.N. Pak and N.G. Ventov, *Russ. J. Phys. Chem., 49* (1975) 1489.
[74] T. Sakata, in N. Serpone and E. Pelizzetti (eds.), *Photocatalysis, Fundamentals and Applications*, Wiley, New York, 1989, p. 319.
[75] O. Enea, A. Ali and D. Duprez, *New. J. Chem., 12* (1988) 27.
[76] E. Pelizzeti and C. Minero, *Electrochim. Acta, 38* (1993) 47.